Supplemental Material for Quantum Phase Gate Capable of Effectively Collecting Photons based on Gap Plasmons Structure

Qi Zhang[a], He Hao[a], Juanjuan Ren[a], Fan Zhang[a], Qihuang Gong[a,b,c,d], and Ying Gu[*a,b,c,d,]

[a]State Key Laboratory for Mesoscopic Physics, Department of Physics, Peking University, Beijing 100871, China
[b]Frontiers science Center for Nano-optoelectronics Collaborative Innovation Center of Quantum Matter, Peking University, Beijing, China
[c]Collaborative Innovation Center of Extreme Optics, Shanxi University, Taiyuan, Shanxi 030006, China
[d]Beijing Academy of Quantum Information Sciences, Beijing 100193, China

1. Calculation of the coupling coefficient in gap plasmons nanostructure

The Ag nanowire provide evanescent vacuum, while placing the AgNC near the nanowire, localized surface plasmons can be excited due to the collective oscillation of free electrons [1]. The electromagnetic field at the nanogap gets stronger than that in homogeneous vacuum as the evanescent wave undergoes exponential decay. That is the principle of coupling coefficient g enhancement. Here we introduce the method of calculating g in our system.

In the electric-dipole approximation, the coupling coefficient g between a single atom and an individual metallic nanoparticle can be represented as [2]

$$g = \frac{\vec{E} \cdot \vec{\mu}}{\hbar} \tag{1}$$

where $\vec{\mu}$ is the transition dipole moment of atom, and $\vec{E}$ denotes the electric field of single excitation. As for the parameter $\vec{E}$, we use the total energy W of AgNC, which is described by the energy-density integration for dispersive media

$$W = \frac{1}{2}\int \frac{\partial}{\partial \omega}[\omega Re\varepsilon(\omega)]|_{\omega=\omega_c}|\vec{E}_t|^2 dV + \frac{1}{2}\int \mu_0 |\vec{H}_t|^2 dV \tag{2}$$

to normalize the corresponding excited electromagnetic mode $\vec{E}_t$, that

$$\vec{E} = \sqrt{\frac{\hbar\omega_c}{W}}\vec{E}_t \tag{3}$$

Therefore, parameters $\vec{\mu}$, ω_c, W and $\vec{E}_t$ are necessary. In the gap plasmons nanostructure we designed, $\vec{\mu} = 0.17$ e·nm for Cs atom [3], others are obtained by our

CONTACT Ying Gu Email: ygu@pku.edu.cn

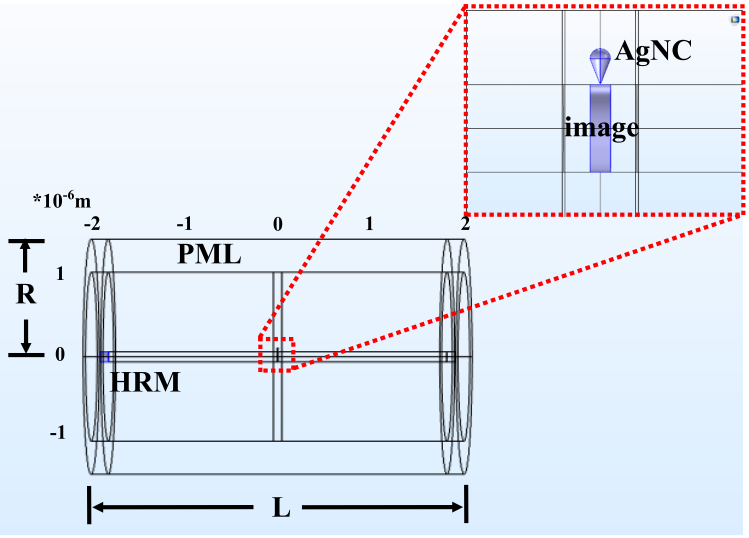

Figure 1 Schematic diagram of the model in COMSOL software. Cylindrical model with length $L = 4$ μm and radius $R = 1.5$ μm surrounding by perfectly matched layer. Purple part on the left side of nanowire is high refractive index material. Inset is the AgNC and its image.

simulation.

We resort to three-dimensional numerical simulation by COMSOL multiphysics software. As shown in Fig. 1, a cylindrical model with length $L = 4$ μm and radius $R = 1.5$ μm is configured. The size of the model is much bigger than those of nanowire and AgNC, leading to changes of model size have little effect on the distribution of electric fields, which is enough to simulate infinite environments. A perfectly matched layer (marked PML in Fig. 1) is introduced to minimize boundary reflections. Meanwhile, to exciting propagating surface plasmons in Ag nanowire, we use a 100 nm high refractive index material at one end of it (marked HRM of nanowire in Fig. 1) thus achieving mode matching to stimulate propagating surface plasmons of nanowire.

Here we describe the methods to obtain several parameters in the above simulation: (1) Resonance frequency ω_c of the cavity. By changing the frequency of the optical source, we obtain the absorption spectra of AgNC with built-in instruction *emw.Qrh*. Fig. 2(c) and 2(d) in the main body of our manuscript show the results. The frequency corresponding to the peak of the curves are ω_c. (2) Total energy W of AgNC. The instruction *emw.Wav* in COLSOL can obtain volume integral of energy directly. It's worth noting that the total energy also includes the image of the AgNC (inset in Fig. 1), because it is produced by the interaction of the AgNC and nanowire. (3) Excited electric field intensity $\vec{E}_t$. Along the axis of symmetry of AgNC, we use *emw.Ei (i=x,y,z)* instruction to get the components of the electric field in each direction of space. Then we need to subtract the background of the evanescent wave to obtain the longitudinal mode of AgNC. So far, the coupling coefficient g can be calculated with these parameters. We compared our results with analytical expressions [4] and had a good agreement.

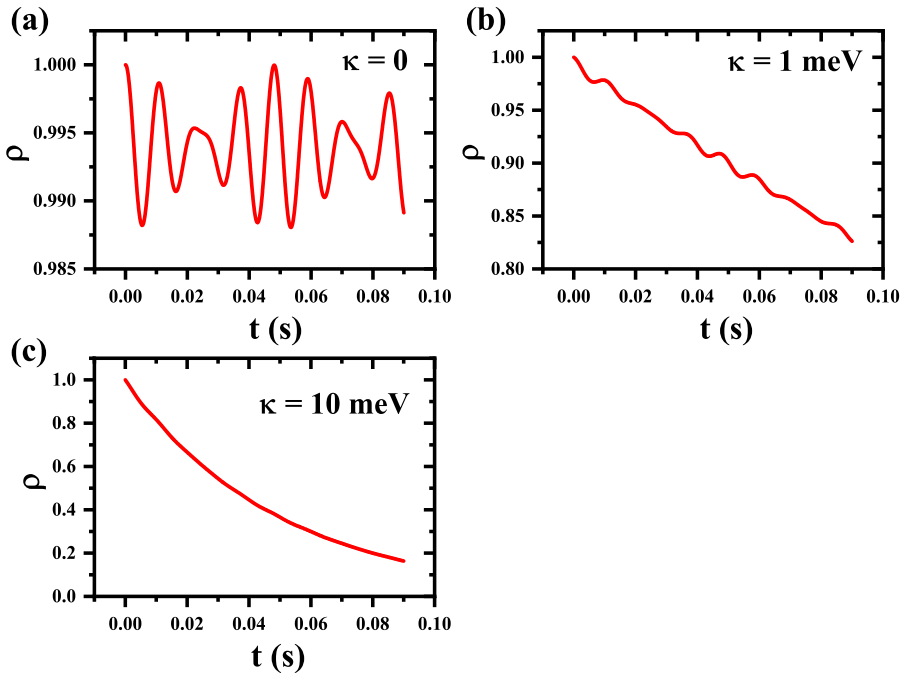

Figure 2 The evolution of matrix elements on the main diagonal in lossless system (a) and lossy system (b) $\kappa = 1$ meV, (c) $\kappa = 10$ meV. In lossless system, $\rho(t)$ oscillates periodically, whereas in lossy system, $\rho(t)$ decays in periodic oscillations.

2. The effect of cavity loss κ on temporal density matrix $\rho(t)$

Fidelity F of the quantum gate is defined by [5]

$$F =< \psi(0)|U^{+}\rho(t)U|\psi(0) > \tag{4}$$

Where temporal density matrix $\rho(t)$ is a crucial parameter that affects the result F. In a cavity, $\rho(t)$ is related to cavity loss κ and atomic spontaneous emission γ. Among them κ dominates because γ is small enough (about 0.1 meV). Here we theoretically explain the effect of cavity loss κ on matrix elements of temporal density matrix $\rho(t)$ and programmatically verify the conclusion.

In 1963, Jaynes and Cummings [6] analyzed the interaction between single-mode electromagnetic field and two-level atom with quantum optics, and proposed well-known J-C model to describe that process. Under the spin wave approximation and the dipole approximation, the Hamiltonian of the system can be expressed as

$$H = \hbar\omega_a\sigma^{+}\sigma + \hbar\omega_c a^{+}a + \hbar g(a^{+}\sigma + \sigma^{+}a) \tag{5}$$

Where ω_a is the atomic transition frequency, ω_c is the frequency of cavity mode, $a(a^{+})$ is annihilation (creation) operator, and $\sigma(\sigma^{+})$ is lowering (raising) operator. The dynamic evolution of the ideal system can be expressed as

$$\dot{\rho} = -\frac{i}{\hbar}[H, \rho] \tag{6}$$

Matrix elements will oscillate periodically. Considering the cavity loss κ and sponta-

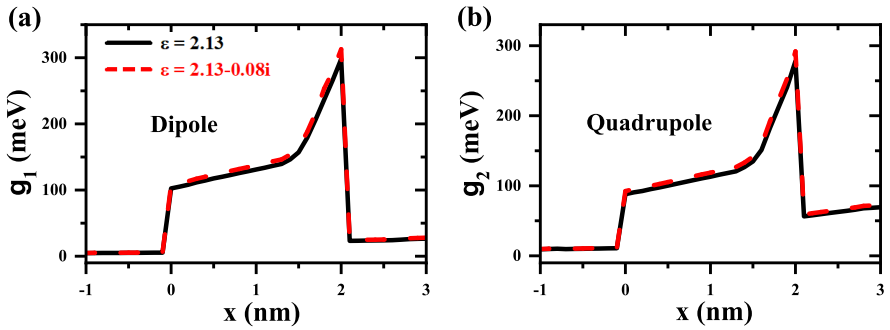

Figure 3 Coupling coefficient g in the nanogap for (a) dipole and (b) quadrupole. Results in SiO_2 (black solid curve) in gain medium with $\varepsilon = 2.13 - 0.08i$ (red dashed curve) are almost the same, where the largest differences between the two curves are 2.1% and 1.7% respectively.

neous emission γ of atom, equation (6) is amended to

$$\dot{\rho} = -\frac{i}{\hbar}[H, \rho] - \frac{\kappa}{2}(a^{+}a\rho - a\rho a^{+} + H.c.) - \frac{\gamma}{2}(\sigma^{+}\sigma\rho - \sigma\rho\sigma^{+} + H.c.) \tag{7}$$

Hence, in actual system, matrix elements temporal density matrix $\rho(t)$ decay with periodic oscillation, the decay rates of matrix elements are proportional to κ and γ.

As for our quantum system, we calculate the matrix element of density matrix at any time though Python software. The module *qutip.mesolve* in package Quantum Toolbox in Python (QuTip) provides solvers for the Lindblad master equation and von Neumann equation [2], which is used in our work. In Fig. 2, we compare in three cases $\kappa_1 = \kappa_2 = 0$ (lossless system), $\kappa_1 = \kappa_2 = 1$ meV and $\kappa_1 = \kappa_2 = 10$ meV, the matrix elements on the main diagonal evolve over time. For simplicity and to exclude the influence of other factors, other parameters are set to $g_1 = g_2 = 100$ meV, $\gamma_1 = \gamma_2 = 0$, $\omega_1 = 2\pi \times 396$ THz, $\omega_2 = 2\pi \times 588$ THz, $\Delta = 0$. Fig. 2(a) shows the evolution of matrix elements in lossless system, which oscillate periodically. As cavity loss κ gets bigger in Fig. 2(b) and 2(c), matrix elements show a trend of gradual decay with time, the bigger the loss, the faster the decay. Even in Fig. 2(c) it decays so fast that we can't see the oscillations. The programming results coincide with the trend of theoretical analysis.

3. Electric field distribution and coupling coefficient affected by gain medium

The introduction of gain medium, on the one hand, can make up the inherent loss of surface plasmons, on the other hand, almost don't affect the distribution of electric field and coupling coefficient. Hence, high fidelity quantum phase gate can be achieved based on our model. Fig. 3 shows the effect on electric field distribution and coupling coefficient of two cavity modes, where the black solid curve stands for results in SiO_2 and red dashed curve for results in gain medium ($\varepsilon = 2.13 - 0.08i$). By comparison, the two red and black cruves are basically the same, the largest differences between them are 2.1% and 1.7% in Fig. 3(a) and 3(b) respectively. From Equ. (1), coupling coefficient g is proportional to electric field intensity E, so electric field intensity have the same trend. Owing to small enough absolute value, g and E almost don't affected by imaginary part of dielectric constant in environment.

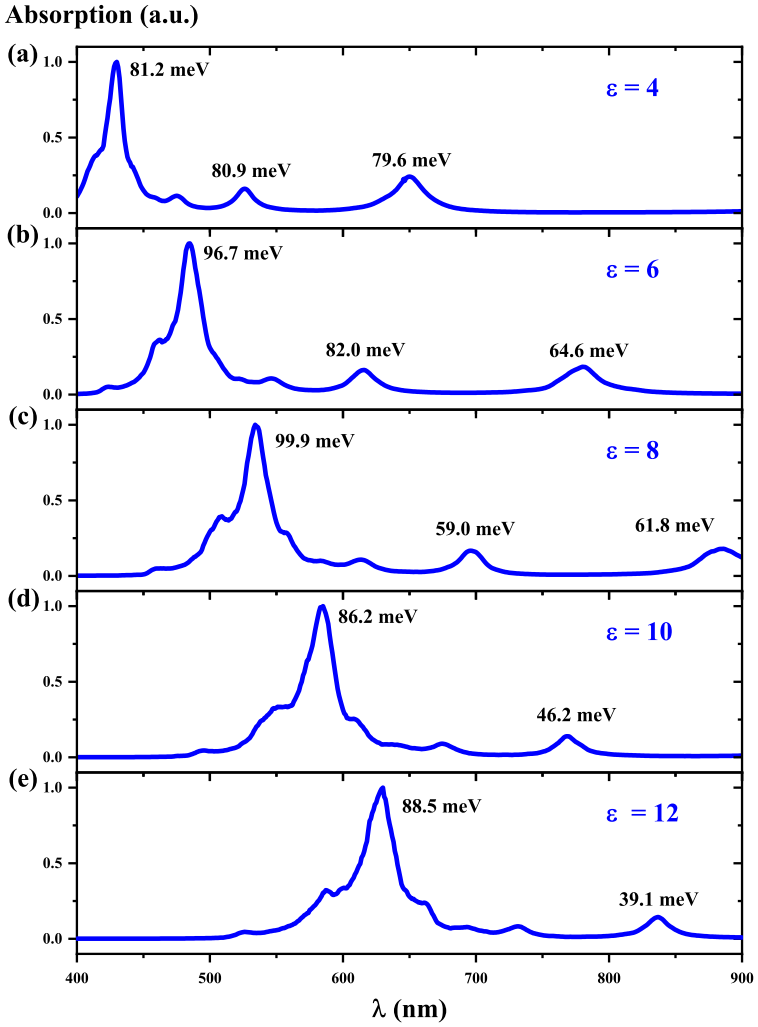

Figure 4 Normalized absorption for AgNC surrounded by high dielectric constant materials. Dielectric constant in environment are (a) $\varepsilon = 4$, (b) $\varepsilon = 6$, (c) $\varepsilon = 8$, (d) $\varepsilon = 10$, and (e) $\varepsilon = 12$. Cavity loss κ is not small enough to realize high fidelity quantum gate.

4. Advantage in size of surface plasmons

Plasmonic structures enable enhanced light-matter interactions at the nanoscale owing to their ultrasmall mode volumes [7, 8]. In recent years, researchers have realized strong coupling based on nanoscale metallic particles theoretically and experimentally. Savasta [9] proposed vacuum Rabi splitting using a single quantum dot in the center of a dimer nanoantenna with $r = 7$ nm. Ren [10] took use of Ag nanorod with $D = 20$ nm, $a = 38.6$ nm to realize reversible photon-exciton coupling and fluorescence collection. Chikkaraddy [11] achieved strong coupling in the nanogap with $d = 0.9$ nm between gold nanosphere and gold nano film. As for our study, the size of the AgNC is also at the nanoscale, which supports ultrasmall localized surface plasmons.

We compare the structures whispering gallery resonators and photonic crystals. In 2003, Vahala [12] pointed out that the sizes of these two structures are usually at the micron scale in his review article. Whispering gallery modes rise from continuous total internal reflection on the boundary between the cavity and the surrounding

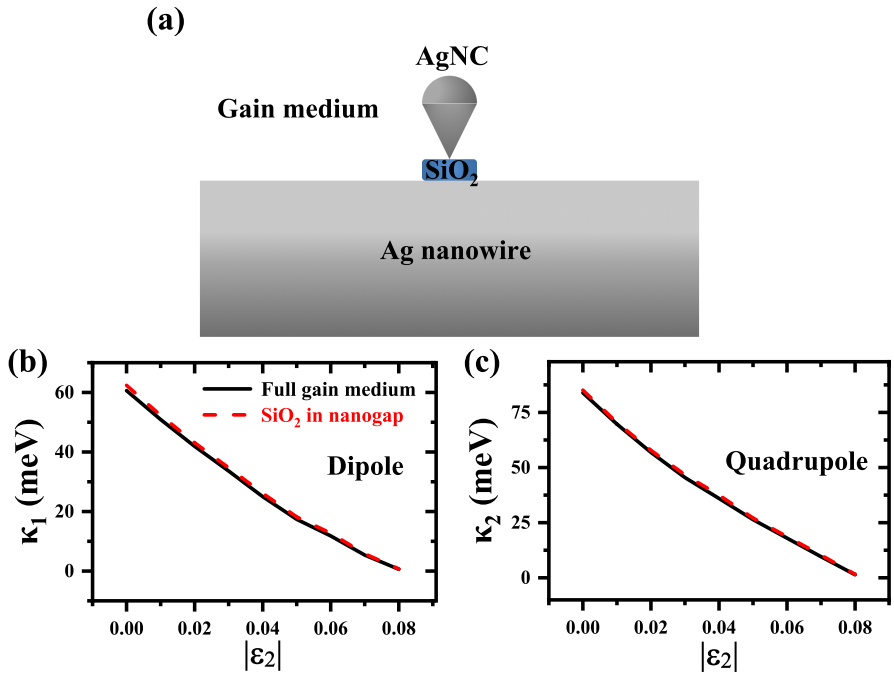

Figure 5 (a) Schematic diagram of the hybrid nanostructure with SiO_2 in nanogap and gain medium in environment. Cavity loss κ varies with imaginary part ε_2 of dielectric constant for (b) dipole and (c) quadrupole. Results in nanostructures with full gain medium (black solid curve) and SiO_2 in nanogap (red dashed curve) are almost the same, where the largest differences between the two curves are 1.5% and 0.7% respectively.

environment [12]. So, the size of the structure is at least in the wavelength order to satisfy the total reflection condition. Previous studies in strong coupling regime based on whispering gallery resonators have proved this view, like microdisk [13], microsphere [14] and microtoroid [15]. Photonic crystals are formed by periodic arrangement of different dielectric constants materials [16]. There are usually several periods in one direction, so the dimensions are not too small. Usually, studies on strong coupling with photonic crystals are also at the micron scale [17–19].

5. Nano-CQED system surrounded by high dielectric constant materials

The proposed system including AgNC surrounded by gain medium is excellent at greatly improving fidelity of quantum gate, though it seems a little speculative. In order to enhance the practicability of the model, we explore a scheme to replace the gain medium with a conventional material with high dielectric constant. The basic nanostructure is the same as shown in Fig. 1(a) in the main body, except for parameter ε changes.

We analyze the mode the AgNC with ε ranges from 4 to 12, the corresponding results are shown in Fig. 4. The figure shows the normalized absorption spectrum at the optical band, where the absorption peaks represent the resonance wavelength and the full width at half-maximum shows the cavity loss [2]. We can see, the resonance frequency of AgNC redshifts with the increase of the dielectric constant. The cavity loss κ maintains on the order of tens of meV, which does not reduce significant. Therefore, we can't increase the fidelity of the quantum gate dramatically.

Although high fidelity quantum gate can't realize, the method still gives us great

enlightenment. In the visible spectrum, there are more than two resonant frequencies on the condition that $\varepsilon = 4, 6, 8$, showing our nano-CQED system surrounded by high dielectric constant materials is expected to be used to implement multi-qubit quantum gates. For example, Chang [20] proposed three-qubit quantum phase gate with combination of three-mode optical cavity and four-level atom based on similar principles. The three-mode gap plasmons nanocavity discussed above may suit for this research. Hence, our research is conducive to the development of on-chip quantum information processing.

6. Results of gain medium in the environment and SiO_2 in the nanogap

Considering the fact that metamaterial-based gain material is difficult to fit the nanogap. We attempt to keep the material in the nanogap SiO_2, and change that in other areas of environment to gain medium. Fig. 5(a) shows the detailed structure around the AgNC. The dielectric constant between AgNC and Ag nanowire is set to $\varepsilon = 2.13$, other material in environment is set to $\varepsilon = 2.13 - 0.08i$. Other parameters are the same as the main body.

We compare the results κ in this case with the main body, results for dipole and quadrupole are shown in Fig. 5(b) and 5(c). κ decreases with ε increases as the gain effect of the material is enhanced. The result under this structure is basically the same as the original manuscript for two cavity modes, indicating that method of gain medium in the environment and normal material in the nanogap can also maintain cavity loss at low level. With $\kappa_1 = 0.7$ meV and $\kappa_2 = 1.6$ meV, final fidelity is 87.1%.

References

[1] H. Raether, *Surface plasmons on smooth and rough surfaces and on gratings*, Springer, 1988, pp. 4–39.
[2] K. Słowik, R. Filter, J. Straubel, F. Lederer and C. Rockstuhl, *Physical Review B*, 2013, **88**, 195414.
[3] A. Lindgård and S. E. Nielsen, *Atomic data and nuclear data tables*, 1977, **19**, 533–633.
[4] E. Waks and D. Sridharan, *Physical Review A*, 2010, **82**, 043845.
[5] C. Ottaviani, S. Rebić, D. Vitali and P. Tombesi, *Physical Review A*, 2006, **73**, 010301.
[6] E. T. Jaynes and F. W. Cummings, *Proceedings of the IEEE*, 1963, **51**, 89–109.
[7] M. S. Tame, K. McEnery, Ş. Özdemir, J. Lee, S. A. Maier and M. Kim, *Nature Physics*, 2013, **9**, 329–340.
[8] Z. Jacob and V. M. Shalaev, *Science*, 2011, **334**, 463–464.
[9] S. Savasta, R. Saija, A. Ridolfo, O. Di Stefano, P. Denti and F. Borghese, *ACS nano*, 2010, **4**, 6369–6376.
[10] J. Ren, Y. Gu, D. Zhao, F. Zhang, T. Zhang and Q. Gong, *Physical review letters*, 2017, **118**, 073604.
[11] R. Chikkaraddy, B. De Nijs, F. Benz, S. J. Barrow, O. A. Scherman, E. Rosta, A. Demetriadou, P. Fox, O. Hess and J. J. Baumberg, *Nature*, 2016, **535**, 127–130.
[12] K. J. Vahala, *nature*, 2003, **424**, 839–846.
[13] K. Srinivasan and O. Painter, *Nature*, 2007, **450**, 862–865.
[14] Y.-S. Park, A. K. Cook and H. Wang, *Nano letters*, 2006, **6**, 2075–2079.
[15] D. Armani, T. Kippenberg, S. Spillane and K. Vahala, *Nature*, 2003, **421**, 925–928.
[16] J. D. Joannopoulos, P. R. Villeneuve and S. Fan, *Nature*, 1997, **386**, 143–149.
[17] T. Yoshie, A. Scherer, J. Hendrickson, G. Khitrova, H. Gibbs, G. Rupper, C. Ell, O. Shchekin and D. Deppe, *Nature*, 2004, **432**, 200–203.

[18] B.-S. Song, S. Noda, T. Asano and Y. Akahane, *Nature materials*, 2005, **4**, 207–210.
[19] X. Gan, K. F. Mak, Y. Gao, Y. You, F. Hatami, J. Hone, T. F. Heinz and D. Englund, *Nano letters*, 2012, **12**, 5626–5631.
[20] J.-T. Chang and M. S. Zubairy, *Physical Review A*, 2008, **77**, 012329.